

# Periorbital Thermal Signal Extraction and Applications

Dvijesh Shastri\*, Panagiotis Tsiamyrtzis\*\* and Ioannis Pavlidis\*

*Abstract*— We propose a novel method that localizes the thermal footprint of the facial and ophthalmic arterial-venous complexes in the periorbital area. This footprint is used to extract the mean thermal signal over time (periorbital signal), which is a correlate of the blood supply to the ocular muscle. Previous work demonstrated that the periorbital signal is associated to autonomic responses and it changes significantly upon the onset of instantaneous stress. The present method enables accurate and consistent extraction of this signal. It aims to replace the heuristic segmentation approach that has been used in stress quantification thus far. Applications in computational psychology and particularly in deception detection are the first to benefit from this new technology. We tested the method on thermal videos of 39 subjects who faced stressful interrogation for a mock crime. The results show that the proposed approach has improved the deception classification success rate to 82%, which is 20% higher compared to the previous approach.

## I. INTRODUCTION

FACIAL physiology changes locally with the onset of stress, either autonomic or non-autonomic. Previous work by Pavlidis et al. have demonstrated that the onset of autonomic stress is associated with instantaneous changes in the blood flow supply of the ocular muscle [1]. Recently, Pavlidis et al. have also demonstrated that the onset of non-autonomic stress is associated with gradual changes in the blood flow supply of the corrugator muscle [2][3]. Heat convected from the flow of ‘hot’ arterial blood in superficial facial vasculature eventually radiates through the skin in the thermal infrared band. Therefore, one can record and analyze these heat signals through a thermal imaging sensor of sufficient sensitivity. The analysis problem depends on the localization of the relevant tissue areas in facial thermal imagery. Consistent tissue localization over time is very important, if one is interested to extract meaningful measurements.

The periorbital tissue of interest is located in the inner corner of the eye, as this is the area that sits atop the facial and ophthalmic arterial-venous complexes, which supply with blood the orbicularis oculi muscle. The proposed periorbital segmentation method has at its core a fuzzy-based segmentation algorithm. This algorithm copes well with the fuzziness characterizing thermal imagery, due to the heat diffusion phenomenon. Manual intervention is limited

to selecting seed pixels in the initial frame of the image sequence. Starting from these operator-selected seed pixels, the algorithm computes new, optimal seed pixels. Then, it uses the computed seed pixels to grow the periorbital segments. Finally, Gaussian filtering applies on the segmented regions.

Pavlidis et al. reported the applicability of the periorbital thermal signature in deception detection [4], [5]. However, their 10% hottest pixels heuristic segmentation approach [6] highly depends on operator expertise. It assumes that only the 10% hottest pixels of a carefully chosen region of interest (ROI) are periorbital. Although the method is simple and easy to implement, its performance heavily depends on the choice of the initial ROI. The periorbital region must coincide with approximately the 10% hottest pixels of the manually selected ROI. If this constraint is violated, the 10% methodology consistently misclassifies captured temperature pixels, as shown in Fig. 1. As a result, inconsistency in the measurement of the periorbital signal is introduced, which is detrimental to final applications such as deception analysis. The method we propose is not bound by the constraints of the heuristic method and the choice of the initial ROI has no effect on the method’s performance.

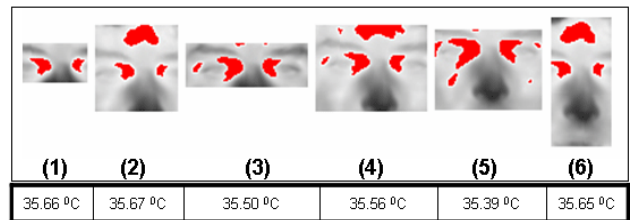


Fig. 1. The 10% hottest pixels heuristic segmentation approach: The algorithm over-segments the periorbital area (red colored) if an inappropriate Region of Interest (ROI) is selected. The problem is evident from the variability of the mean periorbital temperature when different sizes ROIs are selected on the same initial frame.

The remaining paper is organized as follows: In Section II, we present some background information on facial physiology and stress. In Section III, we describe the segmentation, tracking, and noise reduction methods. In Section IV, we show experimental results for the proposed method and compare it to the 10% heuristic method. We also analyze the performance of the proposed method in a deception detection application. Finally, we conclude the paper in Section V.

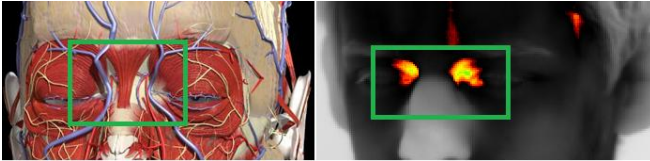
## II. PERIORBITAL REGION AND STRESS

Pavlidis et al. have shown that increased blood flow in the periorbital region is a ubiquitous manifestation of instantaneous stress [1]. When a person is under perceived

\*Dvijesh Shastri and Ioannis Pavlidis are with the Computational Physiology Lab, University of Houston, Houston 77204-30101, Texas, USA {[dshastri@uh.edu](mailto:dshastri@uh.edu) [ipavlidis@uh.edu](mailto:ipavlidis@uh.edu)} \*\*Panagiotis Tsiamyrtzis is with the Dept. of Statistics, Athens Univ. of Economics and Business, 76 Patission Street, 104 34 Athens, Greece [pt@aub.gr](mailto:pt@aub.gr)

threat, the sympathetic division of the autonomic nervous system (ANS) prepares the body accordingly. It tasks the eyes to collect accurate visual information and the brain to process that information quickly. Increased ocular muscle activity requires energy (metabolic fuel), which is carried via increased blood flow. The ophthalmic and facial vessels, which are the predominant supply of blood to the orbicularis oculi muscle, have superficial segments in the inner eye corners (see Fig. 2(a)). Therefore, variable heat dissipation from the periorbital region due to change in blood flow can be monitored through a thermal camera (see Fig. 2(b)).

Our task is to capture the temperature evolution in the periorbital region as accurately as possible and thus, form the periorbital signal to detect elevated instantaneous stress levels.



(a) Periorbital Anatomy [7] (b) Thermal Facial Image

Fig. 2. Anatomical and thermal images of the face

### III. PERIORBITAL SIGNAL EXTRACTION

The periorbital thermal signal extraction has three modules. In module I, the periorbital region is being *segmented*. In module II, the segmented region is being *tracked* frame by frame. In module III, the extracted thermal signal is being *cleaned* from unwanted noise.

#### A. Module I: Segmentation

The proposed segmentation approach has three main steps:

- 1) *Selection of Seed Pixels*: The periorbital segmentation process is initiated by selecting two points in the initial frame, one in each inner eye corner. We then center a  $9 \times 9$  pixel grid on each seed pixel and search for the respective maximum temperature pixels. We repeat this step for every incoming frame and compute new seed pixels based on those from the previous frame. This simple step guarantees labeling of the local maxima as the seed pixels for every incoming frame. In order to avoid convergence of both seed pixels to the same local maximum, we hide the first segmented region by setting its pixel values to zero while computing the second seed pixel location. Thus, the second seed pixel always picks the local maximum in the second periorbital region.

- 2) *Adaptive Fuzzy-Based Segmentation*: Having localized the maximum temperature periorbital pixels, we use them as seeds in the adaptive fuzzy connectedness algorithm [8], [9].

The primary reason for using the fuzzy connectedness algorithm is that thermal images are characterized by the heat diffusion phenomenon and therefore, thermal phenomenology fits well the fuzzy connectedness segmentation framework.

The algorithm calculates fuzzy affinity ( $k$ ) between two pixels based on a weight function that incorporates geometric, temperature homogeneity, and temperature gradient space adjacency:

$$k = \{((c, d), \mu_k(c, d)) \mid (c, d) \in C\}, \text{ and} \quad (1)$$

$$\mu_k : C \times C \rightarrow [0, 1],$$

where,  $C$  is a  $n$ -dimensional array of pixels,  $c$  and  $d$  are pixel locations in an image, and  $\mu_k$  is the strength of the strongest path between  $c$  and  $d$ . The fuzzy affinity of every incoming pixel ( $d$ ) with respect to the seed pixel ( $c$ ) is computed using the following equation:

$$\mu_k(c, d) = \mu_\alpha(c, d) [w_h h(f(c), f(d)) + w_g g(f(c), f(d))], \quad (2)$$

where,  $f(c)$  and  $f(d)$  are the temperature values of pixels  $c$  and  $d$ , respectively. Adaptive weights  $w_h$  and  $w_g$ , are the ratios of the homogeneity ( $h$ ) and the gradient ( $g$ ) functions. Similarity between two pixels is measured by the homogeneity function  $h$ . The function  $g$  determines the gradient energy of the incoming pixel with respect to the seed pixel. The adjacency function  $\mu_\alpha(c, d)$  allows 4-pixel neighborhood.

Once the first periorbital region is grown, we perform a similar growing operation for the other periorbital region in the frame.

- 3) *Gaussian Filtering*: Finally, all the temperature values inside the segmented periorbital regions are smoothed using a Gaussian filter. The filtering is effected using the weighted mean as opposed to the simple mean. The segmented regions fluctuate in size due to the pulsating nature of blood flow in the vessels. Also, blinking alters the segmented regions. The simple mean allows both of these phenomena to interfere in the periorbital signal. Therefore, the weighted mean is necessary to smooth out this unwanted fluctuation. We place a Gaussian mask centered at each seed pixel and compute the weight of every neighboring pixel. Thus, the pixels closer to the seed pixels are weighted more compared to the boundary pixels. This ensures capture of thermal evolution from the core only of the segmented periorbital region.

The entire segmentation process is repeated for every incoming frame.

## B. Module II: Tracking

We employ the coalitional tracker [10], which has been specially designed for tracking facial tissue. It can handle various head poses, partial occlusions, and inter-tissue region temperature variations. On the initial frame, the user initiates the tracking algorithm by selecting a rectangular ROI, which covers the periorbital region. The user also selects two seed pixels, one for each side of the periorbital region, to initiate the periorbital segmentation. The tracker estimates the best matching blocks in the next frame of the thermal clip. Next, the segmentation step takes over the task of localizing the exact periorbital regions. This interleaving of tracking and segmentation steps is iteratively implemented until the end of the image sequence.

## C. Module III: Noise Cleaning

The extracted periorbital signal consists of a low frequency component that represents the long term trend of blood flow levels, and a mid frequency component that is associated with disturbances caused by stress. These components contain valuable information. However, the measurement carries substantial high frequency noise due to imperfections in tissue tracking and segmentation. We use the noise cleaning algorithm that we proposed in [6] to suppress high frequency noise from the signal.

## IV. EXPERIMENTAL RESULTS

### A. Segmentation Performance

We have tested the proposed algorithm on 39 thermal clips. The thermal clips were captured during the interrogation of subjects who were suspects of check stealing in a mock crime scenario [6]. In this section we will compare fuzzy-segmentation results with the 10% hottest pixels method. We employed 6 individuals and asked them to select ROIs on the initial thermal frame of 39 thermal clips. These individuals received basic training on ROI selection before the experiment began. Based on their selections, the periorbital region was segmented via the 10% heuristic and the proposed fuzzy-based approach. Fig. 3 shows segmentation results for one of the subjects.

Unlike the 10% heuristic approach, the fuzzy-based method never over-segments the periorbital region. This guarantees that the signals extracted are true representations of the temperature in the periorbital area. Also, unlike the 10% approach, the new method is not sensitive to the ROI selection. Therefore, regardless of the ROI size, the method segments consistently the periorbital area and produces the same mean temperatures for the same frame, which the 10% method fails to do.

### B. Performance on Deception Detection

Improved measurement technology for the periorbital signal is expected to positively affect deception detection applications that use it. To prove this we used the heuristic and the proposed segmentation methods in combination with a classification algorithm [6], to make comparative deception predictions.

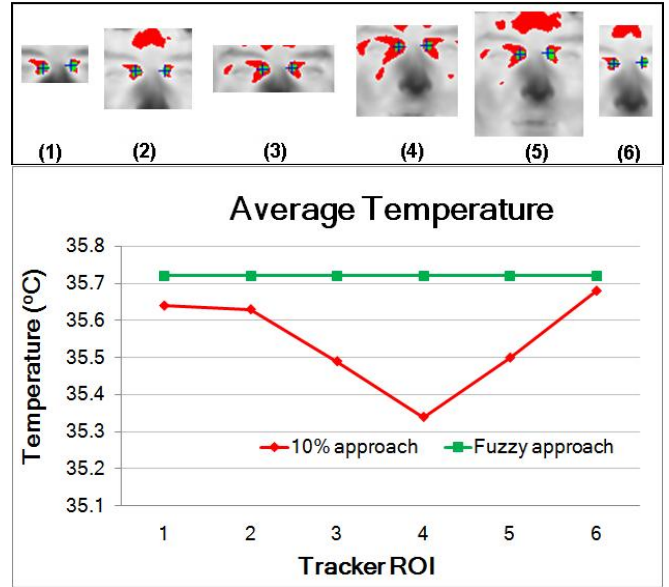


Fig. 3. Comparison of the fuzzy-based (green colored) and 10% (red colored) approaches for periorbital segmentation. The top figure shows visual comparison and the bottom figure shows numerical comparison of both approaches. The crosses in the periorbital regions represent seed pixel positions.

The classification algorithm uses the fact that periorbital temperature variation during an interrogation is the result of the combined stress effect from the interrogation itself, which is present in all subjects, and the deception stress effect, which is present only in deceptive subjects. The interrogation effect is realized as a global ascending trend in the periorbital signal, while the deception effect is transient in nature and appears in deceptive subjects during the critical questions only. Therefore, our prediction scheme compares the rate of the temperature change during a critical question, which was question 4 ( $r_{i4}$ ) in the specific dataset, against the rate of the temperature change during the entire interview ( $R_i$ ), for every subject  $i$ :

$$r_{i4} - R_i \rightarrow \begin{cases} > 0 \text{ subject } i \text{ is D,} \\ \leq 0 \text{ subject } i \text{ is ND.} \end{cases} \quad (3)$$

In other words, if the physiological change in the critical question is greater than the baseline change, then the subject is classified as deceptive (D); otherwise, he/she is labeled non-deceptive (ND). Details about this mock crime experimental design can be found in [6].

We extracted the periorbital signals of 39 subjects four times by selecting the same respective ROIs and then predicted each subject's deception classification for every run. Predicting the subjects more than one time was necessary to avoid the variability that the tracker introduces due to its stochastic component. Fig. 4 illustrates that the fuzzy-based segmentation algorithm outperformed the 10% approach with a considerable margin (approximately 20%)

for all four runs. The results verify the higher application performance of the new algorithm. One may notice small variability in the prediction success rate from run to run in both segmentation approaches (see Fig. 4). As mentioned above, momentary failures in the tracking algorithm cause local temperature variation in the periorbital signal, which, ultimately, alters prediction results for borderline subjects.

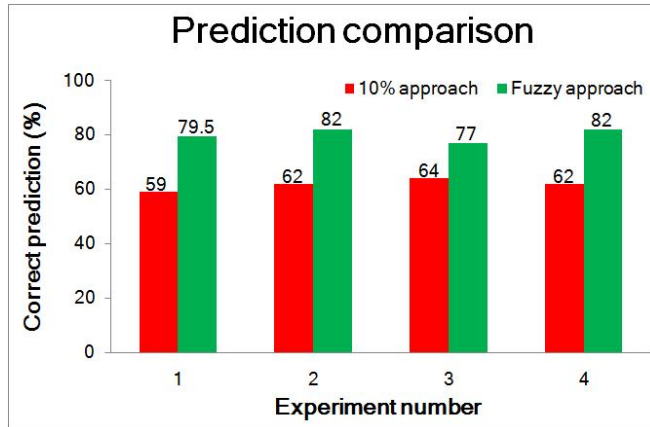


Fig. 4. Comparison of success rates in a deception experiment based on the periorbital signals extracted from the 10% hottest pixels and fuzzy-based approaches.

## V. CONCLUSION

We have proposed a novel method for periorbital tissue segmentation in thermal clips. Within the ROI, the periorbital region is localized using the adaptive fuzzy-based segmentation approach. The experimental results show that the new segmentation approach exhibits performance superior to the 10% hottest pixels heuristic approach. In conclusion, apart from the fact that the fuzzy-based segmentation approach does not require user expertise in ROI selection, it produces accurate and consistent mean temperature, irrespectively of the ROI size. Based on the results from 39 subjects, we conclude that the combination of accurate tissue segmentation, tissue tracking, and noise cleaning along with the appropriate classification algorithm has consistently achieved a deception classification rate close to 80%.

One problem we have noticed with the proposed method is that in some cases, the seed pixels cannot be recovered after momentary tracker failures. This happens only when sub-regions in the ROI, other than the periorbital region, have locally maximum temperatures. For now, we manually reselect the seed pixels for those cases.

Another open issue is the manual selection of the initial seed pixels; an automation solution is forthcoming.

## ACKNOWLEDGMENT

This work was supported by a research contract from the Defense Academy for Credibility Assessment (DACA). Any opinions, findings, and conclusions or recommendations

expressed in this material are those of the authors and do not necessarily reflect the views of the funding agency.

## REFERENCES

- [1] J. Levine, I. Pavlidis, and M. Cooper, "The face of fear," *Lancet*, vol. 357, p. 1757, 2001.
- [2] C. Puri, L. Olson, I. Pavlidis, J. Levine, and J. Starren, "Stresscam: non-contact measurement of users' emotional states through thermal imaging." in *Proceedings of the 2005 ACM Conference on Human Factors in Computing Systems*, Portland, Oregon, April 2-7 2005, pp. 1725-8.
- [3] Z. Zhu, P. Tsiamyrtzis, and I. Pavlidis, "Forehead thermal signature extraction in lie detection", in *Proceedings of the 29<sup>th</sup> Annual International Conference IEEE Engineering in Medicine and Biology Society*, Lyon, France, pp. 243-256, August 2007.
- [4] I. Pavlidis, N. Eberhardt, and J. Levine, "Seeing through the face of deception," *Nature*, vol. 415, p. 35, 2002.
- [5] I. Pavlidis and J. Levine, "Thermal image analysis for polygraph testing," *IEEE Engineering in Medicine and Biology Magazine*, vol. 21, no. 6, pp. 56-64, November-December 2002.
- [6] P. Tsiamyrtzis, J. Dowdall, D. Shastri, I. Pavlidis, M. Frank, and P. Ekman, "Imaging facial physiology for the detection of deceit," *International Journal of Computer Vision*, vol. 71, no. 2, pp. 197-214, October 2006.
- [7] B. J. Moxham, C. Kirsh, B. Berkovitz, G. Alusi, and T. Cheeseman, "Interactive head & neck (CD-ROM)," Primal Pictures, December 2002.
- [8] J. Udupa, and S. Samarasekera, "Fuzzy Connectedness and Object Definition", *SPIE Proceedings Medical Imaging*, volume 2431, pages 2-10. SPIE, 1995.
- [9] A. Pednekar, I. Kakadiaris, and U. Kurkure, "Adaptive Fuzzy Connectedness-Based Medical Image Segmentation", *Proceedings of the Indian Conference on Computer Vision, Graphics, and Image Processing*, pp. 457-462, Ahmedabad, India, December 16-18, 2002.
- [10] J. Dowdall, I. Pavlidis, and P. Tsiamyrtzis, "Coalitional tracking," *Computer Vision and Image Understanding*, vol. 106, no. 2-3, pp. 205-219, May-June 2007.